# Molecular Imaging of Thermochromic Carbohydrate-Modified Polydiacetylene Thin Films

Anna Lio,[†] Anke Reichert,[†,‡] Dong June Ahn,[§] Jon O. Nagy,[†] Miquel Salmeron,[†] and Deborah H. Charych*[,†]

*Lawrence Berkeley National Laboratory, Center for Advanced Materials, Berkeley, California 94720, and Department of Chemical Engineering, Korea University, Seoul 136-701, Korea*

*Received April 21, 1997. In Final Form: July 18, 1997*[⊗]

Polymerized thin films based on polydiacetylenes (PDAs) undergo distinct color transitions that lend themselves to applications in biosensing, surface modification, nonlinear optics, and molecular electronics. The mechanism of the thermochromic blue to red color transition of PDA thin films was investigated at the molecular level using atomic force microscopy and at the macroscopic level with visible absorption and Fourier transform infrared spectroscopy. The thermochromic transition temperature is found to be between 70 and 90 °C. At the molecular level, the ordering of the film *increases* at the thermochromic transition and remains ordered up to temperatures well above the transition (e.g., 130 °C). No evidence for previously suggested entanglement or disordering of the alkyl side chains is observed. The pendant side chains rearrange from a partially disordered configuration characteristic of the blue film, to a well-ordered close-packed hexagonal arrangement in the red form. The rearrangment of the pendant side chains is linked to the formation of the red phase PDA.

## Introduction

The blue to red color transition of polydiacetylenes (PDAs) has inspired researchers for several decades.[1−5,13] These color changes occur in polydiacetylene single crystals, cast films, solutions, and Langmuir−Blodgett (LB) films. They arise from a variety of environmental perturbations including temperature (thermochromism)[3] and mechanical stress (mechanochromism).[4] We have recently demonstrated that biomimetic polydiacetylenes incorporating carbohydrate ligands change color from blue to red upon specific binding of a biological target (biochromism).[5−7] An example of such a lipid−polymer membrane film is shown in Figure 1. The films are composed of 10,12-pentacosadiynoic acid (PCA) and carbohydrate derivatives of PCA (e.g., sialic acid, SA-PCA), and prepared by the Langmuir−Schaefer (LS) technique. The molecular assembly depicted in Figure 1 was designed to mimic the spatial organization and functionalization of natural cell membranes that are similarly "sugar coated". Molecular recognition at the carbohydrate interface is reported as a color change by the conjugated polydiacetylene polymer backbone of alternating triple and double bonds.[6] The color change, typically from blue to red arises from reduction of the effective conjugated length of the polymer ene−yne backbone. Films such as that shown in Figure 1 have been used to detect the binding of influenza virus as this virus normally binds to sialic acid residues on cell surfaces.[8−10] The sialic acid diacetylenic lipid is dispersed in the "matrix" lipid of PCA.

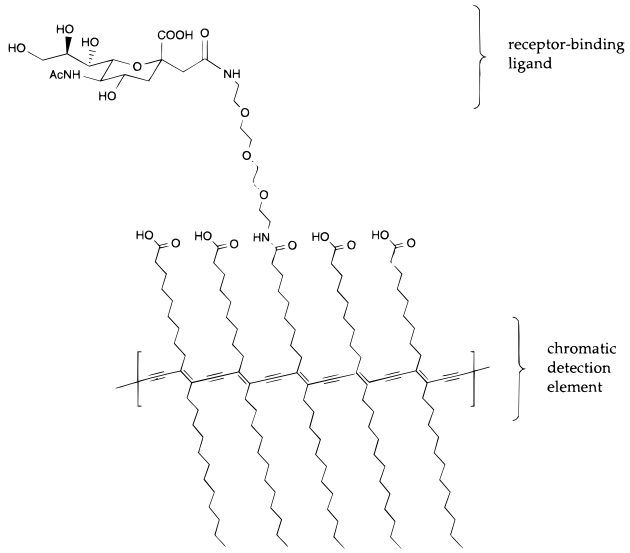


**Figure 1.** Schematic diagram of the carbohydrate-modified molecular assembly used for these studies. The conjugated polymer backbone of alternating double and triple bonds constitutes the chromatic detection element. The sialic acid carbohydrate is a receptor-specific ligand for influenza virus.

In order to fully exploit the use of ligand-modified polydiacetylene films as biosensors, it is necessary to develop a complete molecular-level understanding of the blue to red color transition. In the longer term, an understanding of the molecular mechanisms underlying the optical transition may lead to optimized systems that are responsive to a variety of physical phenomena, as well as chemical and biological agents. To this end, we have

* To whom correspondence should be addressed.
† Lawrence Berkeley National Laboratory.
‡ Present address: BASF-Aktiengesellschaft, Polymer Research, ZKD/B-B1, D-67056, Ludwigshafen, Germany.
§ Korea University.
⊗ Abstract published in *Advance ACS Abstracts,* November 1, 1997.

(1) Bloor, D.; Chance, R. R. *Polydiacetylenes*; NATO ASI Series E; Applied Science; Martinus Nijhoff Publishers: Dordrecht, 1985.
(2) Tieke, M.; Wegner, G. In *Topics in Surface Chemistry*; Kay, E., Bagus, P. S., Eds.; Plenum Press: New York, 1978.
(3) Wenzel, M.; Atkinson, G. H. *J. Am. Chem. Soc.* **1989**, *111*, 6123.
(4) Galiotis, C.; Yong, R. J.; Batchelder, D. N. *J. Polym. Sci. Polym. Phys. Ed.* **1983**, *21*, 2483.
(5) Charych, D. H.; Nagy, J. O.; Spevak, W.; Bednarski, M. D. *Science* **1993**, *261*, 585.
(6) Reichert, A; Nagy, J. O.; Spevak, W.; Charych, D. *J. Am. Chem. Soc.* **1995**, *117*, 829.
(7) Charych, D.; Cheng, Q.; Reichert, A.; Kuziemko, G.; Stroh, M.; Nagy, J. O.; Spevak, W.; Stevens, R. C. *Chem. Biol.* **1996**, *3*, 113.
(8) White, J.; Kielian, M.; Helenius, A. *Q. Rev. Biophys.* **1983**, *16*, 151.
(9) Paulson, J. C. *The Receptors*; Conn, M., Ed.; Academic Press: New York, 1985; Vol. 2, pp 131−219.
(10) Spevak, W.; Nagy, J. O.; Charych, D. H.; Schaefer, M. E.; Gilbert, J. H.; Bednarski, M. D. *J. Am. Chem. Soc.* **1993**, *115*, 1146.

S0743-7463(97)00406-X CCC: $14.00 

begun a program that attempts to investigate the nature of the blue to red transition at the nanoscopic, microscopic, and macroscopic level using a variety of structural and spectroscopic tools. In this paper, we focus on the blue to red transition induced by heat (thermochromism). In subsequent reports, we will attempt to reconcile these results with color transitions induced by specific binding of biomolecules (biochromism), chemical agents, and other physical phenomena such as UV light and mechanical stress.

The precise molecular mechanism of the blue to red color transition is not completely understood, even for the more well-studied thermochromic transition. Numerous investigations on color transitions have relied on data obtained from employing one or two spectroscopic techniques, typically visible absorption[11,12] and resonance Raman spectroscopy.[13−16] These techniques directly probe the polymerized ene−yne chromophoric unit but not the pendant side chain conformation. Other methods such as $^{13}C$ NMR[17,18] can elucidate pendant side chain structure. However, the assignment of specific conformational changes requires the use of synthetic model compounds with known conformation.[19] Taken as a whole, the embodied work on PDA thermochromism suggests two basic threads: (1) the blue to red thermochromic transition is associated with reduction of the effective conjugated length of the ene−yne backbone and (2) the electronic properties of the polymer ene−yne backbone are strongly coupled to pendant side chain conformation. However, many conflicting reports exist, and general principles and rules have yet to be established.[20,21] A few reports in the literature on LB films of PCA have proposed that side chain entanglement and disordering directly affects the backbone conjugation.[12−14] A more detailed and direct *molecular level* probe of side chain group structure during the color transition is desirable to elucidate these effects. Atomic force microscopy (AFM) is particularly suitable for directly investigating the structure and extent of long-range order in the pendant side chain groups.[22] Fourier transform infrared spectroscopy (FTIR) readily provides information about specific functional groups and relative orientational transitions.[3]

The films discussed in this report are different than the typical LB layers. In this case, overcompressed multilayers are formed and transferred onto solid supports. The overcompressed layers provide high coverage and high optical density for visible absorption spectroscopy. Because of the ultimate use of these materials as biomolecular sensors, it was desirable to expose the hydrophilic, biosensitive groups to the interface and to avoid the use of cadmium ions in the subphase. Langmuir−Schaefer (LS) deposition of PDA onto a hydrophobic substrate was found to be suitable for this purpose. The overcompressed multilayers are well-ordered, show very high optical density, and are obtained in a single deposition cycle.

## Experimental Section

**Materials.** 10,12-Pentacosadiynoic acid, PCA, was purchased from Farchan Laboratories and used as received. The synthesis of the C-glycoside of sialic acid and the sialic acid lipid is reported elsewhere.[10,23] *n*-Octadecyltriethoxysilane (OTE) was purchased from Hüls America (Piscataway, NJ) and vacuum-distilled upon receipt. House-distilled water was passed through a four-cartridge Millipore $\mu$QF purification train producing water with resistivity of 18.2 MΩ·cm. All solvents used were spectral quality. All spreading solutions were filtered through a 0.2 $\mu$m nylon or PTFE membrane to remove traces of polymer.

**PDA Film Preparation.** Glass and mica surfaces were made hydrophobic by depositing a monolayer of OTE using a published procedure[24,25] with the additional step of filtering the OTE prehydrolysis solution through an 0.2 $\mu$m nylon or PTFE membrane prior to dilution with cyclohexane. After self-assembly, the OTE samples were sonicated for 30 min to produce cluster-free layers.[26] All substrates were kept under pure cyclohexane prior to LS transfer of the polydiacetylene layers.

The SA-PCA/PCA polydiacetylene films were prepared by spreading a chloroform solution containing 5% SA-PCA and 95 % PCA monomer lipids onto the clean water surface of a standard Langmuir trough (KSV, Finland). After spreading and evaporation of solvent, the films were compressed, typically, to 20 mN/m, and allowed to equilibrate for 30 min (final pressure ca. 12.5 mN/m). The layer was irradiated with 254 nm light from a handheld UV lamp (UVP Mineralight, 30 $\mu$W/cm$^2$) for 1 min. After irradiation, the blue floating polymer is clearly visible to the naked eye. At this point, the hydrophobized substrate is horizontally touched to the water surface, slowly removed and blown dry with a stream of argon or nitrogen. The blue polymer is clearly seen on the substrate surface.

**Visible Absorption Spectroscopy.** Spectra were taken with a Hewlett-Packard 8452A diode array spectrophotometer using a single beam configuration, deuterium lamp, and UV filter at the source output. PCA films on glass were placed inside a 2 mm path length cuvette. Spectra were recorded in air.

**Heat Treatment of Samples.** The blue samples were heated in a vacuum oven for 30 min at each temperature (50, 70, 90, 110, 130 °C). The samples were cooled to room temperature before being characterized.

**Atomic Force Microscopy.** Two different atomic force microscopes were used in this study. Images larger than 1 $\mu$m$^2$ were acquired with a commercially available instrument (Park Scientific Instrument, Sunnyvale, CA). In this case Si Ultralevers, force constant 0.1 N/m (Park Scientific Instrument, Sunnyvale, CA), were used. Commercially available photolithographically patterned glass slides were used to allow imaging of the exact same region of the film after each temperature step (Bellco Glass Inc., Vineland, NJ). Images smaller than 1 $\mu$m$^2$ were taken with a home-built AFM, which has been described previously.[26] In this case silicon nitride cantilevers with a nominal force constant of 0.1 N/m were used (Park Scientific Instruments, Sunnyvale, CA). Both microscopes are operated in contact mode, and in the latter case a four-quadrant photodiode enables the acquisition of topographic and lateral force images *simultaneously*. All measurements were carried out under ambient laboratory conditions.

**Fourier Transform Infrared (FTIR) Spectroscopy.** Spectra were collected with a Perkin-Elmer FTIR 2000 spectrometer equipped with an MCT-A (mercury−cadmium−telluride) detector which was cooled at liquid nitrogen temperature. The spectrometer was purged continuously with dry nitrogen gas to minimize water vapor bands and $CO_2$. Five hundred twelve scans at a resolution of 4 cm$^{-1}$ were coadded in order to achieve a reasonable signal-to-noise ratio. A nonpolarized beam in transmission mode at perpendicular incidence angle was employed.

(11) Mino, N.; Tamura, H.; Ogawa, K. *Langmuir* **1991**, *7*, 2336.
(12) Deckert, A. A.; Fallon, L.; Kiernan, L.; Cashin, C.; Perrone, A.; Encalarde, T. *Langmuir* **1994**, *10*, 1948.
(13) Saito, A.; Urai, Y.; Itoh, K. *Langmuir* **1996**, *12*, 3938.
(14) Batchelder, D. N.; Bloor, D. *Advances in Infrared and Raman Spectrosocopy*; Clark, R. J. H.; Hester, R. E., Eds.; Wiley: Heyden, 1984; Chapter 4.
(15) Smith, B. E. J.; Batchelder, D. N. *Polymer* **1991**, *32*, 1761.
(16) Exarhos, G. L.; Risen, W. M., Jr.; Baughman, R. H. *J. Am. Chem. Soc.* **1976**, *98*, 481.
(17) Beckham, H. W.; Rubner, M. F. *Macromolecules* **1993,** *26*, 5192.
(18) Tanaka, H.; Thakur, M.; Gomez, M. A.; Tonelli, A. E. *Macromolecules* **1987**, *20*, 1987.
(19) Tanaka, H.; Gomez, M. A.; Tonelli, A. E.; Thakur, M. *Macromolecules* **1989**, *22*, 1208.
(20) Chance, R. R. *Macromolecules* **1980**, *13*, 396.
(21) Rubner, M. F.; Sandman, D. J.; Velazquez, C. *Macromolecules* **1987**, *20*, 1296.
(22) Lio, A.; Reichert, A.; Nagy, J. O.; Salmeron, M.; Charych, D. H., *J. Vacuum Sci. Technol., B* **1996**, *14*, 1481.
(23) Nagy, J. O.; Bednarski, M. D. *Tetrahedron Lett.* **1991**, *32*, 3953.
(24) Kessel, C. R.; Granick, S. *Langmuir* **1991**, *7*, 532.
(25) Xiao, X. D.; Liu, G.-Y.; Charych, D. H.; Salmeron, M. *Langmuir* **1995**, *11*, 1600.
(26) Kolbe, W. F.; Ogletree, D. F.; Salmeron, M. *Ultramicroscopy* **1992**, *42−44*, 1113.

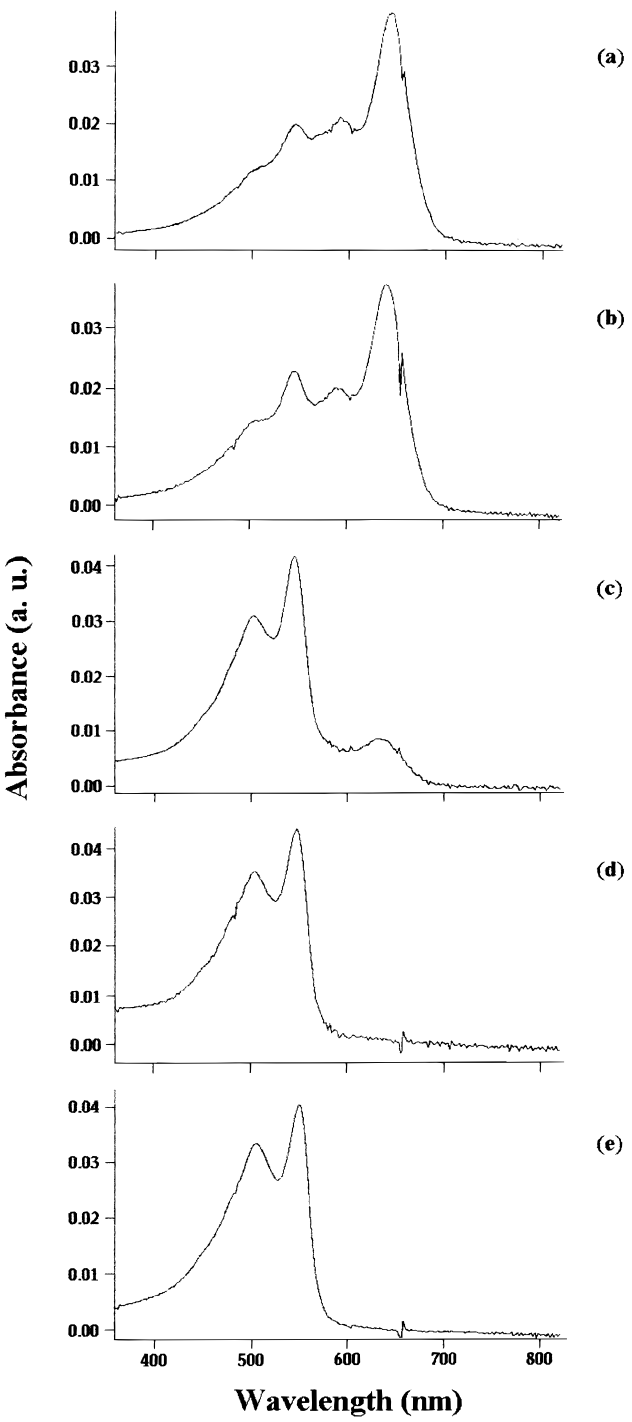


**Figure 2.** Optical absorption spectra for the blue phase films (a) and films annealed at 50, 70, 90, and 110 °C (b−e).

A background single beam spectrum was obtained with a clean glass substrate. Each sample spectrum for the polydiacetylene film on a hydrophobic OTE surface was subtracted by that for the bare OTE surface treated under the same conditions. The transmission spectra showed a typical cutoff below ca. 2200 $cm^{-1}$, since glass substrates were used as sample supports. In order to investigate IR bands related to head groups of the polydiacetylene film (below the cutoff wavenumber), we employed the external reflection mode at a near normal incidence angle (10° off from the surface normal). Use of grazing angle external reflection mode was not helpful for examining head group related bands, because their transition dipole moments are most likely lying parallel to the film surface and are canceled out due to image inversion. After heating, all samples were probed in a sample chamber at room temperature. The IR spectra reported here are raw data.

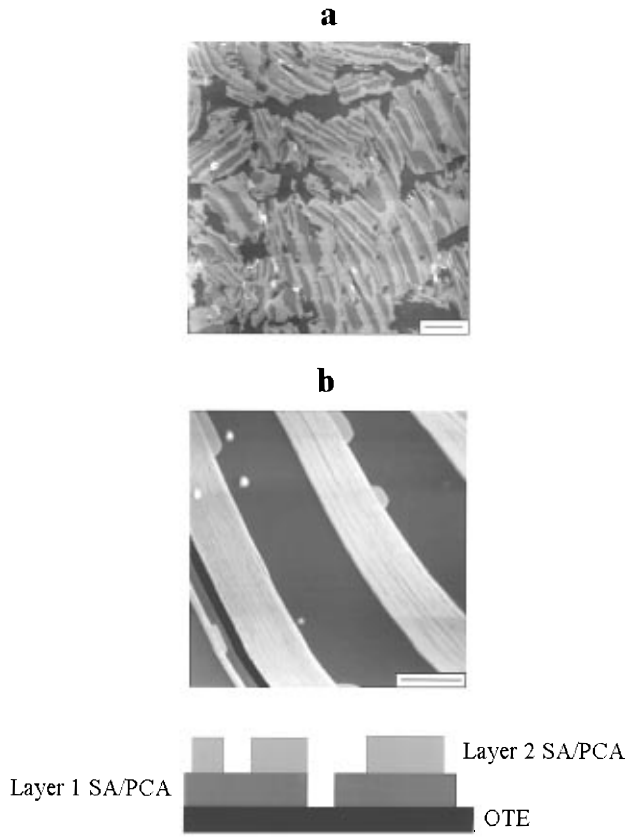


**Figure 3.** AFM images of blue phase films: (a) Micrometer-sized PDA domains are separated by uncovered OTE areas. Scale bar = 5 $\mu$m. (b) Within a single PDA domain a stripelike morphology on top of an almost complete layer (layer **1)** is observed. The thickness of both layer **1** and the stripes corresponds to a trilayer tilted about 35° from the surface normal. Scale bar = 2000 Å.

## Results and Discussion

**Visible Absorption Spectroscopy.** Figure 2 shows the optical absorption spectra obtained at different temperatures (25, 50, 70, 90, 110 °C). The optical absorption spectrum for the blue phase film is shown in Figure 2a. The main excitonic peak of the blue form occurs at 640 nm, with a smaller vibronic maximum occurring at 590 nm. At 25 °C the blue phase film also shows the presence of the red phase, as evidenced by the small but non-negligible absorption at 540 nm. (Note: the term "red phase" traditionally refers to the physical appearance of the material.)

Heat treatment of blue phase films changes the color of the material to red (thermochromism). Optical spectra of heat-treated films are shown in Figure 2b−e. Heating the blue-phase films to 50 °C produces only a slight increase in the red phase peak at 540 nm (Figure 2b). This film appears blue-purple. When the temperature is increased to 70, 90, and 110 °C, the blue phase absorption maximum at 640 nm gradually decreases while the red phase peak at 540 nm increases in intensity (Figure 2c−e). Complete conversion to the red phase for the films described occurs at temperatures between 70 and 90 °C.

**Characterization of the Blue Phase Films: Morphology and Molecular-Level Structure.** Despite the fact that overcompressed multilayers were used to make the films, they are of well-defined morphology at the microscopic level and are highly ordered at the molecular level. Figure 3a shows a 35 × 36 $\mu m^2$ AFM image of a blue phase film transferred on to OTE/glass. Micrometer sized striped domains of increased height (medium to bright regions) are separated by darker (reduced height)

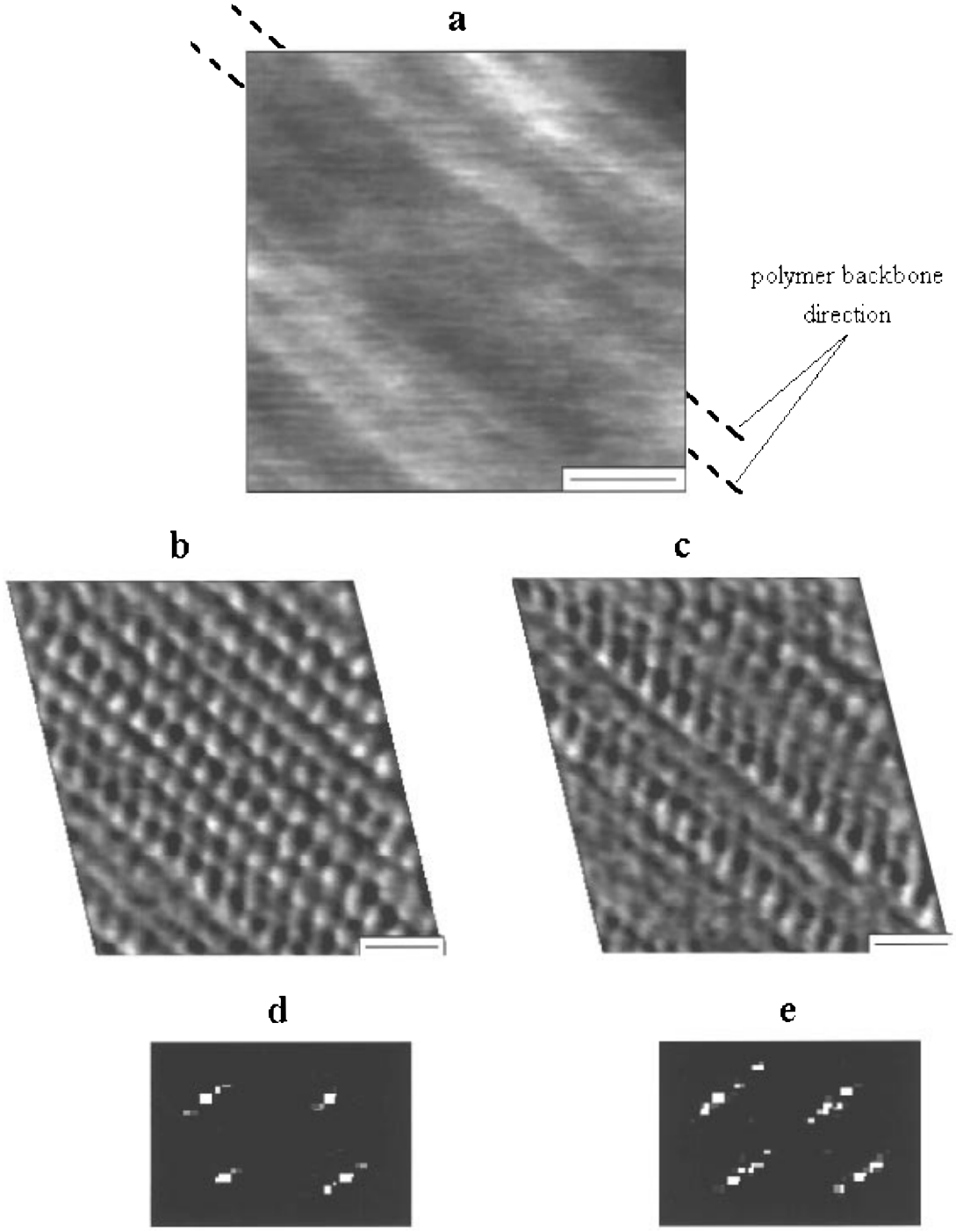


**Figure 4.** (a) AFM images of blue phase layer **1**. Very fine striations parallel to one another are visible. Scale bar = 200 Å. (b and c) Molecular scale frictional force images taken within the area shown in (a). Scale bar = 10 Å. (d and e) 2D-FFT spectra relative to (b) and (c), respectively.

regions. Zooming in on the darkest regions between the domains reveals the characteristically featureless morphology of the underlying OTE layer.[26] The dark OTE regions could be subjected to irreversible wear by the AFM tip until the mica substrate was reached. At this point, the depth of the newly formed hole was measured to about 25 Å, corresponding to the thickness of a single OTE layer.[25,27] The medium to bright striped domains in Figure 3a are regions of the SA-PCA/PCA film (hereafter referred to simply as SA/PCA film) separated by the dark featureless OTE layer. The striped morphology of the domains suggests height differences corresponding to more than one layer of the SA/PCA film within a given domain. The brightest stripes appear to form on top of a relatively uniform SA/PCA film (that is, uniform at this magnification and within that particular domain). We will refer to the uniform SA/PCA film as layer **1** and to the brightest, striped overlayer as layer **2.** The bright stripes of layer **2** within each SA/PCA domain run parallel to each another. However, different orientations are observed in different domains as seen in Figure 3a. Figure 3b shows a higher magnification AFM image of a single SA/PCA domain. The stripes of layer **2** are actually composed of well-packed chords that run parallel to the direction of the stripe itself.

Higher magnification scans (1000−2000 Å) of layer **1** also reveal very fine striations (Figure 4a). They are seen

(27) Wasserman, S. R.; Whitesides, G. M.; Tidswell, I. M.; Ocko, B. M.; Pershan, P. S.; Axe, J. D. *J. Am. Chem. Soc.* **1989**, *111*, 5852.

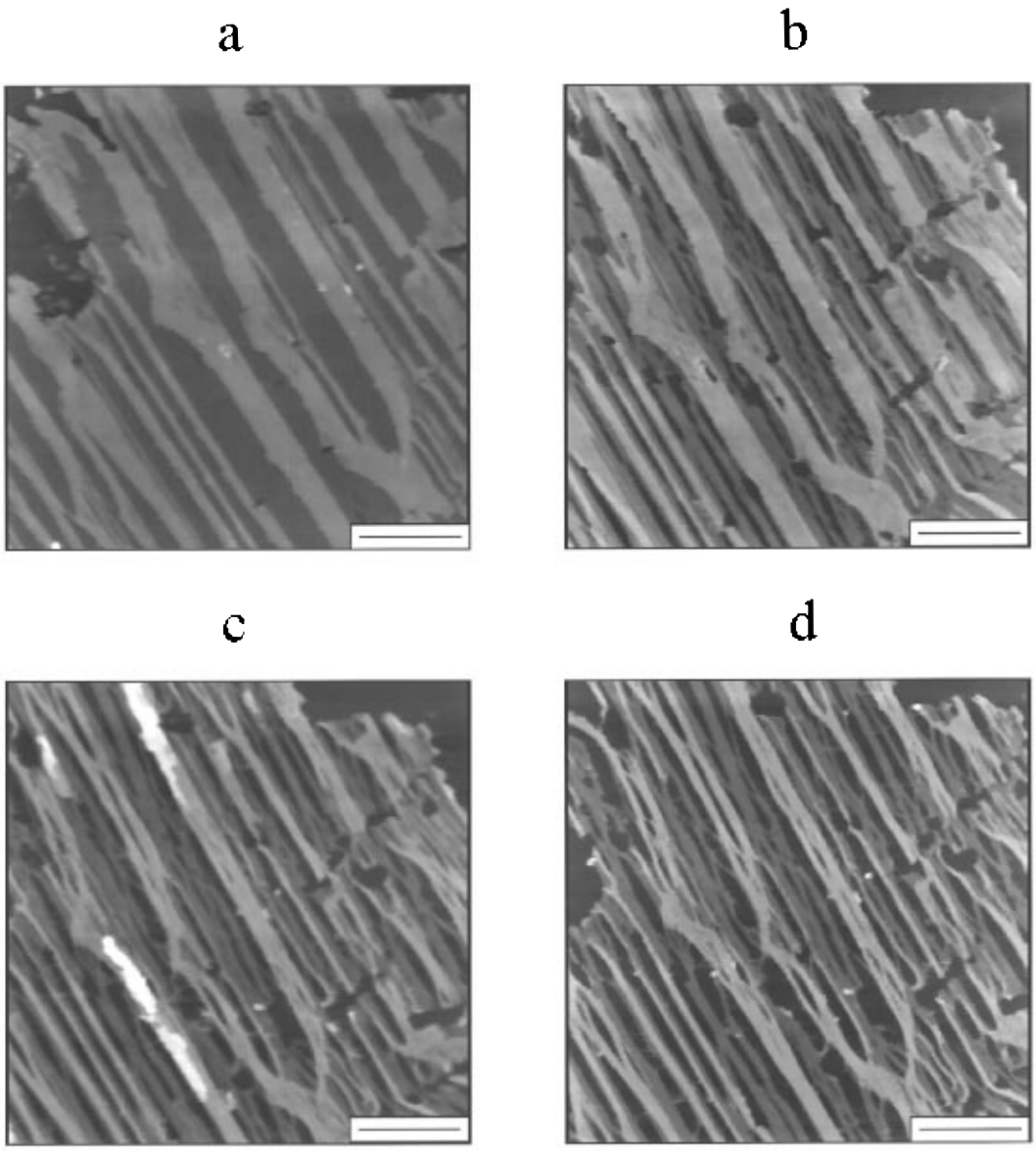


**Figure 5.** AFM images of a SA/PCA film on OTE/glass as a function of annealing temperature: (a) no heating (blue phase); (b) 70 °C, 30 min; (c) 90 °C, 30 min; (d) 110 °C, 30 min. The same area of the film was imaged after each heating cycle. Scale bar = 2 $\mu$m. Upon annealing, layer **1** starts to separate parallel to the direction of the polymer backbone into fine fibers. The process starts from the holes and cracks that already existed in the layer.

to be parallel to one another as well as to the stripes. The roughness across them is measured to be 2−3 Å. These areas of the SA/PCA film are relatively robust. In fact, repeated scanning at low load (1−5 nN for tip radii 200−400 Å) does not cause any damage.

The heights of layer **1** and layer **2** determined from the AFM images are 79 ± 8 and 78 ± 8 Å, respectively. On the basis of molecular models, the length of a PCA molecule is estimated to be 32 Å. Therefore, the measured thickness of each layer (∼78 Å) corresponds to a trilayer of PCA tilted about 35° from the surface normal. This value for the tilt angle is close to the one determined by X-ray reflectivity measurements for multilayers of Cd salts of the same PCA molecule.[28,29] The same thickness was measured by AFM for films of 100% PCA prepared under the same conditions. These results suggest that the flexible sialic acid portion of the molecule (comprising 5% of the film) does not contribute to the measured height.

Molecular resolution images are routinely obtained on layer **1** at low load values. Parts b and c of Figure 4 show two molecular resolution frictional force images acquired in the area shown in Figure 4a. The corresponding 2D-FFT (fast Fourier transform) power spectra are also shown (Figure 4d,e). These images indicate that while the film as a whole is ordered at the molecular level, the highest degree of order exists in the direction parallel to the striations of layer **1** (Figure 4a). The lattice constant, *a*, along this direction, as measured both from real-space images and corresponding 2D-FFTs, is 4.8 ± 0.5 Å. This value agrees well with the spacing between molecules along the polydiacetylene backbone as measured by electron diffraction (4.90 Å).[28,30] Therefore, it is reasonable to conclude that the direction of the striations of layer **1** represents the direction of the polymer backbone.

A lower degree of order exists between parallel polymer chains, probably due to random mismatch between neighboring polymer chains with respect to one another (Figure 4b,c). Furthermore, the variation in contrast

(28) Lieser, G.; Tieke, B.; Wegner, G. *Thin Solid Films* **1980**, *68*, 77.
(29) It also agrees with AFM results obtained by us on Cd-PDA monolayers deposited on mica.
(30) Day, D.; Lando, J. B. *Macromolecules* **1980**, *13*, 1483.

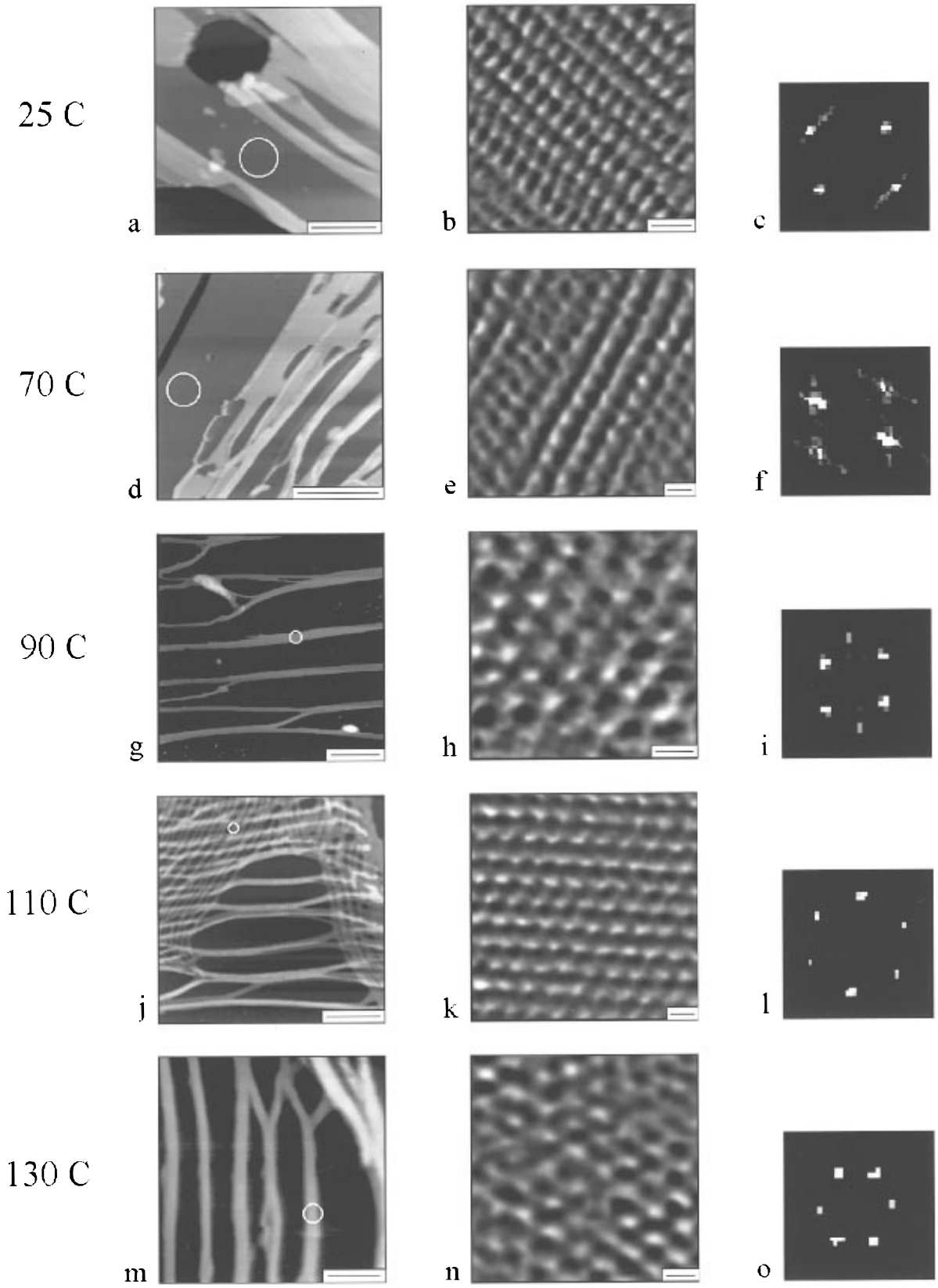


**Figure 6.** Representative AFM images for a series of heat-treated red phase films deposited on OTE on mica: (a−c) no heating (blue phase); (d−f) 70 °C, 30 min; (g−i) 90 °C, 30 min; (j−l) 110 °C, 30 min; (m−o) 130 °C, 30 min. Molecular scale pictures (middle column) are frictional force images obtained on the corresponding areas shown in the first column. The last column shows the 2D-FFT spectra relative to the images in the middle column. Scale bars: 2000 Å (a, d, g, j, m); 10 Å (b); 5 Å (e, h, k, n).

visible in Figure 4c may be due to misalignment of the hydrocarbon planes. Molecular resolution images of the blue film on the stripes (layer **2**) are difficult to obtain, often resulting in formation of a hole in the film.

**Characterization and Structure of Heat-Treated Red Phase Films.** Figure 5 shows the micrometer-sized morphology of the SA/PCA films on glass upon heating. As before, the darkest regions are the OTE layers, the brighter region is layer 1, and the brightest stripes are layer 2 (see Figure 3). After each temperature step, it was possible to return to the exact same area of the sample by using commercially available photolithographically

**Table 1. Summary of Spectroscopic and Structural Data Obtained for SA/PCA Films upon Heat Treatment for 30 Min[a]**

| | $\nu_a(CH_2)$ | | $\nu_s(CH_2)$ | | | |
|---|---|---|---|---|---|---|
| temp (°C) | intensity[b] | position[c] ($cm^{-1}$) | intensity[b] | position[c] ($cm^{-1}$) | side chain structure[d] | film color[d] |
| 25 | 0.0032 | 2917.4 | 0.0023 | 2848.8 | partially ordered | blue |
| 50 | 0.0034 | 2917.0 | 0.0022 | 2848.6 | partially ordered | blue-purple |
| 70 | 0.0038 | 2916.4 | 0.0023 | 2848.3 | partially ordered | pink |
| 90 | 0.0037 | 2916.3 | 0.0022 | 2848.2 | ordered | pink |
| 110 | 0.0037 | 2916.4 | 0.0022 | 2848.3 | ordered | dark pink |
| 130 | 0.0034 | 2916.5 | 0.0019 | 2848.4 | ordered | dark pink |

[a] Spectra and images were obtained after cooling to room temperature. [b] ±0.0001. [c] ±0.1. [d] Based on the ability to obtain molecular resolution AFM images which reveal periodic structures, Figure 6. [e] See also visible absorption spectra, Figure 2.

patterned glass slides. The film's morphology and response to temperature were identical whether it was deposited on glass or mica substrates.

Heating the film to 50 °C changes the color from blue to blue-purple as indicated by the optical absorption spectra in Figure 2b. However, the morphology of the film is very similar to that of the blue film (Figure 5a) except for the formation of a few more cracks in layer **1.** The stripes remain parallel to one another within a given domain.

At 70 °C, the film is distinctly purple and more cracks appear in layer **1** in the direction parallel to the polymer (Figure 5b). Since the same region of the film was imaged at this temperature, it is seen that the increased breakage of layer **1** originates at points where cracks and holes already existed in the blue film (compare to Figure 5a). The breakage exposes the dark underlying OTE layer. Heating the film to 90 °C produces yet more cracks (Figure 5c), and the film is now completely in the red form. The cracking of the film ultimately leads to separation of the film into fine, flexible fibers. These flexible fibers of polymer easily bend and sometimes form a netlike structure that can extend for several micrometers (see Figure 6j). Repeated scanning at low loads over any film region in the red phase does not result in any damage suggesting that the film was toughened by the annealing process.

The step heights measured from AFM images for the red phase films indicate that the layer thickness increases about 15% with respect to the blue phase films for both layers. Previous small angle X-ray scattering measurements have determined an approximately 10% increase in the layer thickness for red polymerized Cd-PCA multilayers.[28]

Figure 6 depicts both the microscopic and nanoscopic behavior of the films at 25, 70, 90, 110, and 130 °C, shown from top to bottom, respectively. The left column of images shows the details of single SA/PCA domains at larger scale, whereas the middle column indicates the corresponding molecular scale images. The corresponding 2D-FFT spectra are shown in the third column. The series of images reveals that the thermochromic transition is characterized not only by large scale morphological changes but also by significant changes in the molecular-level structure. At the nanoscopic scale, films heated to 50 and 70 °C (both represented by Figure 6e) are similar to the blue films (Figure 6b). After conversion to the red phase (parts h, k, and n of Figure 6) the AFM images reveal a well-ordered structure with clear hexagonal periodicity, as shown by the corresponding 2D-FFT spectra. From the 2D-FFT, the lattice constant is measured to be 5.0 ± 0.5 Å. By comparison to parts g, j, and m of Figures 6, it is found that one of the crystal axes remains parallel to the direction of the polymer backbone (i.e., the direction of the fibers).

The molecular-scale images show that the thermally-induced color change is accompanied by dramatic changes

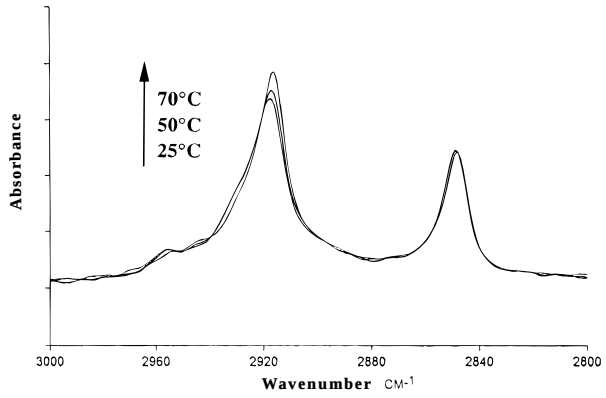


**Figure 7.** Transmission FTIR spectra (CH stretch region) for a series of heat-treated SA/PCA films (25, 50, 70 °C). (Remaining data are found in Table 1.)

in microscopic and nanoscopic film structure. At the molecular level, it appears that the pendant side chains reorganize into a completely ordered structure that is maintained even after annealing the films to temperatures well above the thermochromic transition.

**FTIR Spectroscopy.** In Figure 7, the transmission FTIR spectra of the $CH_2$ symmetric and asymmetric stretch are shown at increasing temperatures. As the SA/PCA film is heated to 70 °C, the peak intensity for the asymmetric methylene stretching band ($\nu_a(CH_2)$) at ca. 2917 $cm^{-1}$ increases by 14 ± 5% of the initial value (Table 1). The peak position also shifts to lower wavenumber. The peak intensity for the symmetric methylene stretching band ($\nu_s(CH_2)$) at 2848 $cm^{-1}$ changes little as the SA/PCA film is heated up to 110 °C. Its peak position also remains nearly constant throughout the heat treatment. The intensity increase of the asymmetric stretch can be explained by reorientation of the pendant alkyl side chains toward the surface normal. As the transition dipole moment of the methylene stretching band becomes parallel to the surface and to the electric field of the IR beam, its peak intensity should increase. The amount of intensity increase upon heating is roughly consistent with the AFM results of increased film thickness (i.e., 15%). The fact that the intensity increases only in the asymmetric methylene band and not in the symmetric one can be explained if the alkyl side chains undergo a rotation about a methylene C−C bond pendant to the ene−yne backbone. Such a rotation brings the C−C−C plane of the pendant alkyl side chain toward the surface normal without dramatically affecting the direction of the transition dipole moment for the symmetric stretch.[13,31,32] Such a rotation is supported by previous studies of the thermochromic transition of polydiacetylene, wherein NMR spectroscopy was used to determine that rotation of the C−C bond $\beta$

(31) Berman, A.; Ahn, D. J.; Lio, A.; Salmeron, M.; Reichert, A.; Charych, D. H. *Science* **1995**, *269*, 515.
(32) Ahn, D. J.; Berman, A.; Charych, D. H. *J. Phys. Chem.* **1996**, *100*, 12455.

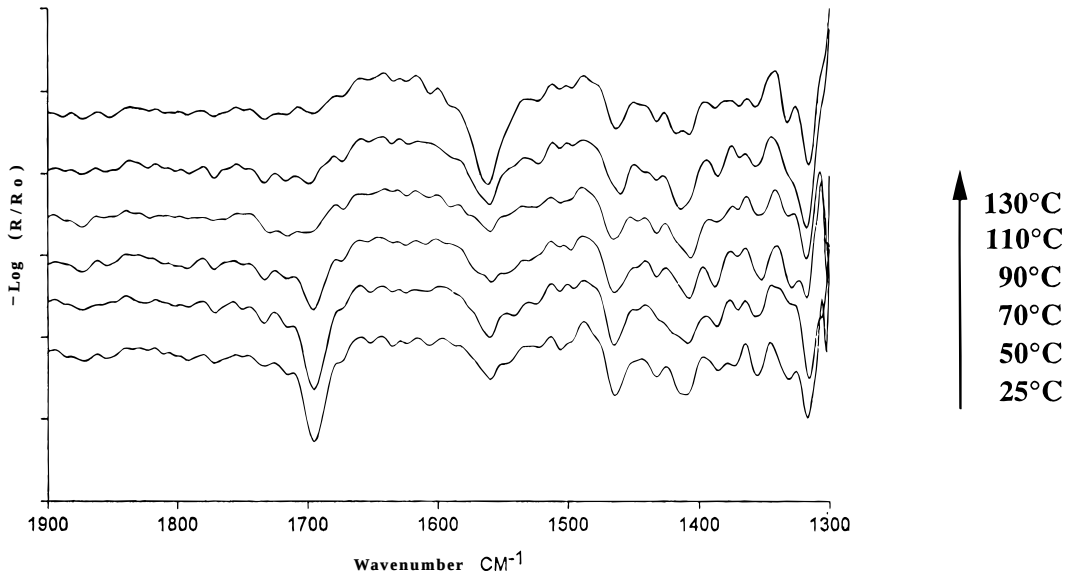


**Figure 8.** Near normal external reflection FTIR (C═O stretch region) spectra for a series of heat-treated SA/PCA films (25, 50, 70, 90, 110, and 130 °C).

to the polymer is directly linked to the color transition.[19] The low-frequency shift of $\nu_a$ suggests more trans character for the alkyl side chain.

The head group region of the SA/PCA film is also readily observed in the near-normal external reflection spectra as shown in Figure 8. Initially at 25 °C, the carbonyl band ($\nu$(C═O)) is observable at 1696 $cm^{-1}$, indicating strong hydrogen bonding in the carboxylic acid head groups, similar to Langmuir−Blodgett films of fatty acids.[33] The peak appearing at 1562 $cm^{-1}$ is assigned to the CNH group of the sialic acid head group. Also observable is the scissoring band of the methylene group at 1465 $cm^{-1}$. As the SA/PCA film is converted to the red phase, the carbonyl stretching band decreases and broadens, indicating that hydrogen bonding in the head group is maintained although somewhat reduced in the red phase at this temperature.[34−37]

**Thermochromic Transition.** It is generally accepted that the red form of the polymer arises from reduced effective conjugated length of the ene−yne polymer backbone.[19,20,38,39] This arises from a planar to nonplanar conformation of the conjugated system.[40] It is also generally accepted that the effective conjugated length is influenced by the pendant side groups. Several studies have suggested that the pendant side chains become entangled and undergo an order to disorder transition as the film changes from the blue to red form.[12,13] Others have suggested that a gauche to trans conformational transition of the methylene groups pendant to the polydiacetylene backbone strains the backbone and results in the color change.[19,41] The molecular scale AFM images in Figure 6 suggest that the side chains do not become disordered in the red phase and actually become more ordered as shown by the 2-D FFT. Therefore, side chain disorder and entanglement can be ruled out as a mechanism of the blue to red transition in these films. In order to determine whether the sialic acid groups were responsible for the ordering effect, we also examined the more "typical" system consisting of a Langmuir−Blodgett monolayer of the cadmium salt of PCA (Cd-PCA). This system has been used extensively in studies of thermochromism. Molecular scale images of Cd-PCA heated to 110 °C also do not show any evidence of disordering of the side chains.[42]

The polymer backbones, composed of conjugated double and triple bonds, are planar in the blue phase films.[43] $^{13}C$ NMR analysis by Tanaka et al.[44] of Poly(ETCD) (R = $(CH_2)_4OCONHCH_2CH_3$ the substitution pendant to the PDA backbone) single crystals indicates that the $CH_2$ carbons $\beta$ and $\gamma$ to the polymer backbone have more gauche character in the blue form. The AFM images of the blue form (Figure 4b−e) reveal irregular packing of the alkyl chains between parallel polymer chains. Upon heating, the side chains clearly reorganize into a near-perfect hexagonal packing (Figure 6). This fact, coupled with the increased intensity of $v_a(CH_2)$ and the low-frequency shift in the FTIR spectra, strongly suggests that the alkyl side-chain bonds have more trans or planar character in the red phase in agreement with the $^{13}C$ NMR data[41] which show a 2 ppm downfield shift of the $\beta,\gamma$-$CH_2$ chemical shifts.[44] The FTIR data obtained from the headgroup region of the film show that hydrogen bonding is maintained in the red form. Hydrogen bonding may lock the headgroups such that the gauche−trans conformational change of the alkyl side chain imposes a strain on the polymer backbone.[45,46] Theoretical calculations have indicated that very slight rotations around the C−C bond of the polymer backbone (5°) are enough to produce a dramatic decrease in the $\pi$-electron conjugation length,[40,47] predicting the blue shift in the visible absorption spectra. The images reveal that despite the morphological changes of the films at the micrometer-scale, the nano-

(33) Kimura, F.; Umemura, J.; Takenaka, T. *Langmuir* **1986**, *2*, 96.
(34) Mino, N.; Tamura, H.; Ogawa, K. *Langmuir* **1991**, *7*, 2336.
(35) Walters, G.; Painter, P.; Ika, P.; Frisch, H. *Macromolecules* **1986**, *19*, 888.
(36) Naselli, C.; Rabolt, J. F.; Swalen, J. D. *J. Chem. Phys.* **1985**, *82*, 2136.
(37) Rabe, J. P.; Rabolt, J. F.; Brown, C. A.; Swalen, J. D. *J. Chem. Phys.*, **1986**, *84*, 4096.
(38) Chance, R. R.; Baughman, R. H.; Muller, H.; Eckhardt, C. J. *J. Chem. Phys.* **1977**, *67*, 3616.
(39) Kolmer, C.; Sixl, H. *J. Chem. Phys.* **1988**, *88*, 1343.
(40) Orchard, B. J.; Tripathy, S. K. *Macromolecules* **1986**, *19*, 1844.
(41) Beckham, H. W.; Rubner, M. F. *Macromolecules* **1993**, *26*, 5198.
(42) Lio, A.; Berman, A.; Charych, D. To be submitted for publication in *Langmuir*.
(43) Orchard, B. J.; Tripathy, S. K. *Macromolecules* **1986**, *19*, 1844.
(44) Tanaka, H.; Gomez, M. A.; Tonelli, A. E.; Thakur, M. *Macromolecules* **1989**, *22*, 1208.
(45) Eckhardt, H.; Boudreaux, D. S.; Chance, R. R. *J. Chem. Phys.* **1986**, *85*, 4116.
(46) Rubner, M. F.; Sandman, D. J.; Velazquez, C. S. *Macromolecules* **1987**, *20*, 1296.
(47) Dobrosavljevic, V.; Stratt, R. M. *Phys. Rev. B* **1987**, *35*, 2731.

scopic order is preserved and actually increases at temperatures well beyond the thermochromic transition. The results indicate that for PDA thin films, hydrogen bonding and conformational transition of the pendant alkyl side chain are associated with the thermochromic transition, in agreement with models suggested by Rubner[41,48] and Tanaka[44] for PDA single crystals.

## Conclusion

Detailed spectroscopic and nanoscopic structural analyses were carried out on ligand-functionalized PDA thin films to obtain a better molecular-level understanding of the blue to red thermochromic transition. It was found that the complementary techniques of AFM, FTIR, and visible absorption spectroscopies provide a reasonably complete visual and spectroscopic picture of the color transition process. AFM probes the molecular ordering and morphology of the polymeric assembly, most notably the pendant side chain groups. FTIR provides information about the relative orientation of specific functional groups in the side chains and visible absorption spectroscopy probes the electronic structure of the chromophore (polydiacetylene backbone).

In the red phase PDA, the chains assume a near-perfect hexagonal packing and the films are thicker with respect to the blue form. Although the micrometer-scale morphology of the SA/PCA film changes dramatically compared to the uniform striped morphology of the blue form, the molecular-scale ordering of the alkyl side chains is actually increased at the transition point and remains ordered at temperatures well beyond the thermochromic transition. The alkyl side chains assume a more all-trans planar configuration, and hydrogen bonding is maintained in the headgroup region, possibly straining the PDA conjugated backbone. These results do not indicate any evidence of alkyl side chain disordering and suggest the importance of molecular-level characterization in conjunction with macroscopic methods. Continued molecular-level studies of these unique lipid−polymer membranes will aid the development of these materials for a variety of scientific and practical applications.

**Acknowledgment.** This work is supported by the Director, Office of Energy Research, Office of Basic Energy Science, Materials Sciences and Energy Biosciences Divisions of the U.S. Department of Energy under the Contract Number DE-AC03-76SF00098 and in part by the Office of Naval Research, Order No. N00014-95-F-0099, through the U.S. Department of Energy under Contract DE-AC03-76SF00098. A. Lio acknowledges partial financial support by the Commission of the European Communities. A. Reichert acknowledges partial financial support by Deutsche Forschungsgemeinschaft (DFG). D. J. Ahn thanks the Korea Science and Engineering Foundation (KOSEF) for financial support through the Exchange of Scientists program. We also thank Dr. Mark Alper, Program Director of the Center for Advanced Materials, Biomolecular Materials Program, for his continued support of this research and Dr. Ulrich Jonas for his critical reading of this manuscript.

LA970406Y

(48) Rubner, M. F.; Sandman, D. J.; Velazques, C. S. *Macromolecules* **1987**, *22*, 1215.